Contents list available at IJRED website

International Journal of Renewable Energy Development

Journal homepage: https://ijred.undip.ac.id

Research Article

Theoretical study of a double-slope solar still with solar air heater condenser

Ahmed Ghazy*

Mechanical Engineering Department, College of Engineering, Jouf University, Sakaka, Al-Jouf, Saudi Arabia

Abstract. Despite their limited water production and efficiency, double-slope solar stills are an appropriate solution for water scarcity in hot arid regions. Numerous studies have focused on enhancing the effectiveness of double-slope solar stills. In this context, this study introduces a double-slope solar with a solar air heater condenser (DSSS-SAHC). The back cover of a conventional double-slope solar still was replaced by a glass air heater in order to recover the still's thermal losses in heating air. The transient performance of the DSSS-SAHC was investigated numerically under real weather conditions and compared to the performance of a conventional double-slope solar still (CDSSS) with the same aspects. The impact of various weather and operation factors on the DSSS-SAHC performance was investigated at air flows of 0.01 and 0.1 kg/s to account for both natural and forced air circulation, respectively. The results revealed an increase of about 15% and 6% in the thermal efficiency of the DSSS-SAHC over that of the CDSSS, respectively, at air flows of 0.1 and 0.01 kg/s despite the DSSS-SAHC distillate was insignificantly greater than that of the CDSSS at both air flows. In addition, the water distillate of the DSSS-SAHC increased as the solar irradiance increased, the ambient wind and ambient temperature had contrary effects on the efficiency, and the initial saline water level had a negligible impact on the overall performance.

Keywords: Double-slope; Solar still; Solar air heater; Thermal performance.

Received: 25th April 2023; Revised: 14th August 2023; Accepted: 5th Sept 2023; Available online: 14th Sept 2023

1. Introduction

Solar desalination has emerged as the optimal method to tackle the water crisis, especially in arid rural areas, and to mitigate the climate-damaging effects of fossil fuels used to drive other desalination technologies. Solar stills, in particular, provide a straightforward, and cost-effective approach to distilling salty water with minimal operational and maintenance costs. These thermal desalination techniques include passive solar stills that solely use solar energy in evaporating salty water, and active solar stills that utilize additional thermal energies. An enormous amount of research work has been devoted to evaluating and enhancing the performance of various active and passive solar stills. For instance, Mevada *et al.* (2022) increased the distillate production of a conventional solar still (CSS) by 1.1 kg/m^2.day by using sensible energy storage materials. Elgendi *et al.* (2022) optimized the pyramid still performance by feeding water automatically to the still. Alwan *et al.* (2020) increased the productivity of a CSS by about 292% by heating saline water in an external collector and incorporating a hollow rotating cylinder within the still to increase the evaporation area. Modi *et al.* (2020) studied the effect of various initial water masses on the performance of a spherical basin solar still with a parabolic reflector. Kabeel *et al.* (2020) investigated the performance of a tubular still combined with parabolic concentrators. Using modified artificial neural networks, Essa *et al.* (2020) increased the predicted productivity of active solar still by 53.2%. Taamneh *et al.* (2020) studied the performance of an inclined solar still combined with a spiral-tube solar water heater. Fallahzadeh *et al.* (2020) integrated a spiral collector, bubble injector, and copper coil to a solar still in order to boost water evaporation and condensation, respectively. By incorporating a black wick belt driven by a DC motor and rotated horizontally and vertically within the still, Abdullah *et al.* (2019) increased CSS water production by 315% with nanoparticles and by 300% without them. Tabrizi *et al.* (2010) predicted that the daily production of a cascade weir-type solar still would decrease from 7.4 kg/m^2.day, at a minimum water flow rate, to 4.3 kg/m^2.day, at a maximum water flow rate. Sathyamurthy *et al.* (2020) increased the daily yield of stepped solar still by 34.2% by coating its absorber plate with black paint containing 20% fumed silicon oxide nanoparticles.

Passive basin-style solar stills are the most affordable and easy solar stills to construct, operate, and maintain. This makes them an excellent choice for rural areas with limited manufacturing and maintenance resources. Although single-slope solar stills are popular and commonly used, they are more effective in colder climates than in warmer ones. In contrast, double-slope solar stills (DSSS) perform better than single-slope solar stills in hot climates, but in cold climates, they produce less than single-slope ones. (Tiwari *et al.*, 1986). The distillate yield of DSSS was compared to those of single slope solar still (SSSS) and pyramid solar still (PSS) (Ahmed *et al.*, 2014). They experimentally observed that the daily distillate of DSSS was 3.95 L, compared to 3.6 L for SSSS and 4.25 L for PSS. In addition, the distillate yield of DSSS decreased with increasing the water mass in the basin (Murugavel *et al.*, 2010 and

* Corresponding author
Email: aeghazy@ju.edu.sa (A. Ghazy)

https://doi.org/10.14710/ijred.2023.53928
ISSN: 2252-4940/© 2023.The Author(s). Published by CBIORE

Murugavel & Srithar, 2011). Moreover, the tilt angle of the glass covers of DSSS plays a key role in determining the thermal performance of the still by governing the amount of solar energy transmitted through the covers. In this regard, El-Maghlany (2015) explored the optimal tilt angles of the two DSSS covers for various latitudes. He concluded that the optimal tilt angle for each cover depends on the south orientation of that cover and that the optimal tilt angles of two covers are not necessarily equal. Furthermore, Castillo-Tellez *et al.* (2015) investigated the impact of wind velocity on the water production and thermal efficiency of DSSS and concluded that a wind velocity of 3.5 m/s is considered an optimum.

Several research studies have concentrated on improving the efficiency of DSSS. For example, Murugavel *et al.* (2008) compared the effects of using different wick and porous materials in the basin of a DSSS on its yield. They discovered that stills with black light cotton were the most productive ones. Murugavel *et al.* (2010) studied the effect of employing various sensible heat storage materials in the basin of DSSS on its productivity. Raihananda *et al.* (2021) developed a double-slope floating still with a wick absorber for coastal communities. Modi & Jani (2021) increased the daily distillate output of a DSSS by 47.4% by affixing circular hollow fins to the basin plate. Patel *et al.* (2020) modified a DSSS by incorporating transparent side walls and an external reflector. Kumbhar (2019) experimentally investigated the efficiency of a DSSS with and without Paraffin wax PCM and an external reflector. Morad *et al.* (2015) evaluated the performance differences between active and passive DSSS with intermittent cover cooling. The study revealed that the productivity and thermal efficiency of the active still were 29% and 41%, respectively, greater than those of the passive still. Maheswari *et al.* (2022) examined the possibility of replacing the glass cover in DSSS with a transparent PVC sheet. They realized that water condensate adheres to the PVC cover, reducing the sunlight received by the still and, as a result, decreasing the still distillate in comparison to DSSS with a glass cover. By incorporating partially submerged wick segments and fully submerged hollow fins, Modi *et al.* (2022) increased the distillate yield of DSSS by approximately 8.6% and 9.4%, respectively. Zayed *et al.* (2023) increased the distillate output of DSSS by about 49.6% by replacing the flat basin with a prismatic one covered with linen wicks. Dwivedi and Tiwari (2010) compared the thermal and exergy efficiencies of passive and active DSSS. They concluded that passive DSSS has a greater thermal efficiency than active DSSS, but that active DSSS has a greater exergy efficiency. Hussen *et al.* (2023) increased the distillate yield and efficiency of DSSS by about 40% by elevating the basin and employing PCM mixed with nanoparticles. Hedayati-Mehdiabadi *et al.* (2020) increased the water productivity and exergy efficiency of DSSS by 11% and 27%, respectively, by incorporating a PV/T collector to preheat saline water and a PCM to allow the still to produce water overnight. Agrawal & Singh (2021) studied the influence of saline water depth on the performance of DSSSs equipped with PCM and steel wool fiber.

Enhancing the condensation of water vapor within the still has a significant impact on its productivity. In this context, Fath & Hosny (2002) tilted the back wall of a DSSS in order to remain in the shade so that it could serve as a built-in condenser. Nevertheless, the thermal losses from the condenser to the ambient environment, which are unavoidable for the distillation, account for a large portion of the energy input to the still. The recovery of a portion of these losses can significantly boost the thermal efficiency of the still (Rajaseenivasan & Murugavel, 2013 and Belhadj *et al.*, 2015).

In this study, the unavoidable thermal losses from the back glass cover of a DSSS to the ambient environment were partially recovered in air heating, which will significantly improve the overall thermal efficiency of DSSS as a whole. Specifically, the back glass cover of a DSSS was replaced with a glass solar air heater condenser (SAHC) to comprise a double-slope solar still with a solar air heater condenser (DSSS-SAHC). The DSSS-SAHC is suitable for providing distillate water for residence and agricultural usages, as well as hot air for space heating and crop drying. The thermal performance of the DSSS-SAHC was investigated numerically under weather conditions of Sakaka, Saudi Arabia (located at 29.9° N, 39.8° E) and compared to that of an identical conventional double-slope solar still (CDSSS). The impact of both natural and forced circulation on the performance of the DSSS-SAHC was taken into account. The influence of a variation in weather conditions such as solar intensity, ambient temperature, and ambient wind speed, and operation parameters such as air flow rate and initial basin water level on distillate productivity and air heating within the DSSS-SAHC was investigated.

2. Methodology

2.1 System Description

Figure 1 depicts the schematic diagram of the DSSS-SAHC in comparison to a CDSSS with the same basin size. The DSSS has a 1 m × 0.5 m basin made of 3 mm thick galvanized steel. The inner surface of the basin was black coated to maximize the absorption of solar energy, while the outer surface was insulated by an extruded polystyrene board 5 cm thick. The glass covers of the still are 3 mm thick window glass and were tilted 30 degrees in the horizontal plane, which is equal to the latitude angle of Sakaka, Saudi Arabia, in order to maximize incident solar irradiance normal to the glass cover. The glass covers were fixed at 0.1 m above the basin and sealed to avoid water vapor leakage. The SAHC is a 0.5 m × 0.05 m glass channel made from a 3 mm thick window glass sheet that replaced the back glass cover of the basin. The thermophysical properties of the components of the DSSS-SAHC are listed in Table 1. Water

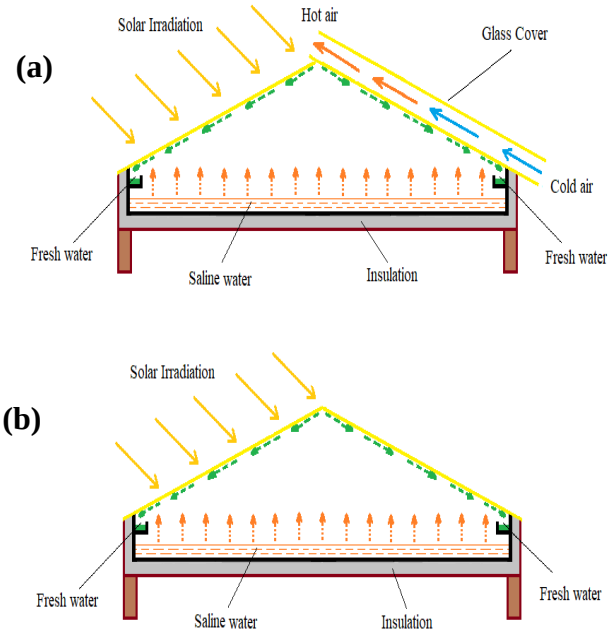

Fig 1. Scheme of (a) DSSS-SAHC, (b) CDSSS.

Table 1
The thermophysical properties of the DSSS-SAHC components.

Property	Glass cover	Basin	Insulation
Density (kg/m^3)	2700	2707	30
Specific heat (kJ/kg.K)	0.840	0.896	1.500
Thermal conductivity (W/m.K)	0.78	204	0.025
Transmissivity	0.87	0.0	0.0
Absorptivity	0.05	0.9	0.1

distillate is condensed inside the still on the front glass cover and the back SAHC, and collected in bottles outside of the still. Ambient air is drawn inside the SAHC either naturally or using a DC fan where it is heated by recovering the condensation energy of the distillate.

2.2 Energy Analysis of CDSSS and DSSS-SAHC

The energy analysis of the DSSS-SAHC in comparison to that of the CDSSS is illustrated in Fig 2. The energy analysis for the cover (g1) of both stills is identical; however, the energy stored in the cover (g2) of the CDSSS is lost to the ambient environment, whereas it is partially recovered by the airflow in the DSSS-SAHC.

The expression for the energy equation of the glass cover (g_1) in the DSSS-SAHC and the CDSSS is

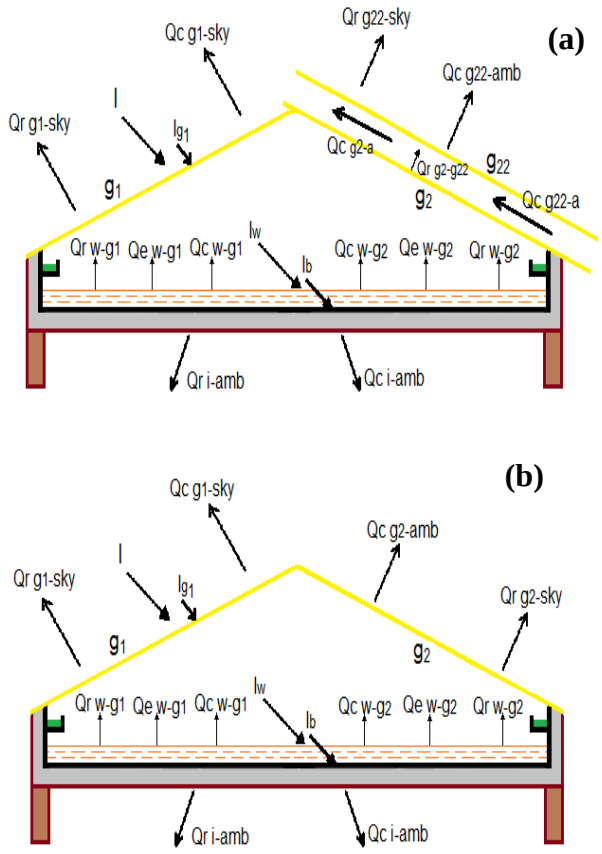

Fig 2. Energy analysis of (a) DSSS-SAHC, (b) CDSSS.

$$m_{g1}\, C_{g1}\frac{dT_{g1}}{dt} = S_{g1} + Q_{R,\,sw\text{-}g1} + Q_{C,\,sw\text{-}g1} + Q_{e,\,sw\text{-}g1} - Q_{R,\,g1\text{-}sky} - Q_{C,\,g1\text{-}amb} \quad (1)$$

where, S_{g1} is the absorbed portion of solar energy by the cover (g_1), $Q_{R,\,sw\text{-}g1}$ is the radiation heat transfer for the saline water in the basin to the cover (g_1), $Q_{C,\,sw\text{-}g1}$ is the convection heat transfer from the saline water to the cover (g_1) through the air inside the still, $Q_{e,\,sw\text{-}g1}$ is the convection mass transfer from the saline water to the cover (g_1) through the air inside the still, $Q_{R,\,g1\text{-}sky}$ is radiative losses from the cover (g_1) to the sky, and $Q_{C,\,g1\text{-}amb}$ is the convective losses from the cover (g_1) to the surrounding ambient, which are defined as follows.

$$S_{g1} = \alpha_g\, I A_{g1} \quad (1a)$$

$$Q_{R,\,sw\text{-}g1} = \sigma\, \varepsilon_{sw}\, F_{g1}\, A_b\, (T_{sw}^4 - T_{g1}^4) \quad (1b)$$

$$Q_{C,\,sw\text{-}g1} = h_{sw\text{-}g1}\, A_b\, (T_{sw} - T_{g1}) \quad (1c)$$

$$Q_{e,\,sw\text{-}g1} = h_e\, A_b\, (P_{sw} - P_{g1}) \quad (1d)$$

$$Q_{R,\,g1\text{-}sky} = \sigma\, \varepsilon_g\, A_{g1}\, (T_{g1}^4 - T_{sky}^4) \quad (1e)$$

$$T_{sky} = 0.0552\, T_{amb}^{1.5} \quad (1f)$$

$$Q_{C,\,g1\text{-}amb} = h_{g1\text{-}amb}\, A_{g1}\, (T_{g1} - T_{amb}) \quad (1g)$$

The energy equation of the glass cover (g_2) in the CDSSS is

$$m_{g2}\, C_{g2}\frac{dT_{g2}}{dt} = Q_{R,\,sw\text{-}g2} + Q_{C,\,sw\text{-}g2} + Q_{e,\,sw\text{-}g2} - Q_{R,\,g2\text{-}sky} - Q_{C,\,g2\text{-}amb} \quad (2)$$

while the energy equation of the glass cover (g_2) in the DSSS-SAHC

$$m_{g2}\, C_{g2}\frac{dT_{g2}}{dt} = Q_{R,\,sw\text{-}g2} + Q_{C,\,sw\text{-}g2} + Q_{e,\,sw\text{-}g2} - Q_{R,\,g2\text{-}g22} - Q_{C,\,g2\text{-}a} \quad (3)$$

where, $Q_{R,\,sw\text{-}g2}$ is the radiation heat transfer from the saline water to the cover (g_2), $Q_{C,\,sw\text{-}g2}$ is the convection heat transfer from the saline water to the cover (g_2) through the air inside the still, $Q_{e,\,sw\text{-}g2}$ is the convection mass transfer from the saline water to the cover (g_2) through the air inside the still, $Q_{R,\,g2\text{-}sky}$ is radiative losses from the cover (g_2) to the sky, $Q_{C,\,g2\text{-}amb}$ is the convective losses from the cover (g_2) to the surrounding ambient, $Q_{R,\,g2\text{-}g22}$ is the radiation heat transfer between the covers (g_2) and (g_{22}), and $Q_{C,\,g2\text{-}a}$ is the convection heat transfer from the cover (g_2) to the flowing air inside the SAHC, which are defined as follows.

$$Q_{R,\,sw\text{-}g2} = \sigma\, \varepsilon_{sw}\, F_{g2}\, A_b\, (T_{sw}^4 - T_{g2}^4) \quad (3a)$$

$$Q_{C,\,sw\text{-}g2} = h_{sw\text{-}g2}\, A_b\, (T_{sw} - T_{g2}) \quad (3b)$$

$$Q_{e,\,sw\text{-}g2} = h_e\, A_b\, (P_{sw} - P_{g2}) \quad (3c)$$

$$Q_{R,\,g2\text{-}sky} = \sigma\,\varepsilon_g\,A_{g2}\,(T_{g2}^4 - T_{sky}^4) \tag{3d}$$

$$Q_{C,\,g2\text{-}amb} = h_{g2\text{-}amb}\,A_{g2}\,(T_{g2} - T_{amb}) \tag{3e}$$

$$Q_{R,\,g2\text{-}g22} = \frac{\sigma\,A_{g2}\,(T_{g2}^4 - T_{g22}^4)}{\frac{2}{\varepsilon_g} - 1} \tag{3f}$$

$$Q_{C,\,g2\text{-}a} = h_{g2\text{-}a}\,A_{g2}\,(T_{g2} - T_a) \tag{3g}$$

Additionally, most of the thermal energy absorbed by the glass cover (g_{22}) in the DSSS-SAHC is transferred to the airflow by convection and to the surrounding environment by convection and radiation as follows.

$$m_{g22}\,C_{g22}\frac{dT_{g22}}{dt} = Q_{R,\,g2\text{-}g22} - Q_{C,\,g22\text{-}a} - Q_{R,\,g22\text{-}sky} - Q_{C,\,g22\text{-}amb} \tag{4}$$

where, $Q_{C,\,g22\text{-}a}$ is the convection heat transfer from the cover (g_{22}) to the flowing air inside the SAHC, $Q_{R,\,g22\text{-}sky}$ is radiative losses from the cover (g_{22}) to the sky, and $Q_{C,\,g22\text{-}amb}$ is the convective losses from the cover (g_{22}) to the surrounding ambient, which are defined as follows.

$$Q_{C,\,g22\text{-}a} = h_{g22\text{-}a}\,A_{g22}\,(T_{g22} - T_a) \tag{4a}$$

$$Q_{R,\,g22\text{-}sky} = \sigma\,\varepsilon_g\,A_{g22}\,(T_{g22}^4 - T_{sky}^4) \tag{4b}$$

$$Q_{C,\,g22\text{-}amb} = h_{g22\text{-}amb}\,A_{g22}\,(T_{g22} - T_{amb}) \tag{4c}$$

The energy equation of the flowing air within the DSSS-SAHC is

$$m_a\,C_a\frac{dT_a}{dt} = Q_{C,\,g2\text{-}a} + Q_{C,\,g22\text{-}a} \tag{5}$$

The energy analysis for the saline water in the basins of both stills is as follows.

$$m_{sw}\,C_{sw}\frac{dT_{sw}}{dt} = S_{sw} + Q_{C,\,b\text{-}sw} - Q_{C,\,sw\text{-}g1} - Q_{C,\,sw\text{-}g2} - Q_{e,\,sw\text{-}g1} - Q_{e,\,sw\text{-}g2} - Q_{R,\,sw\text{-}g1} - Q_{R,\,sw\text{-}g2} \tag{6}$$

$$m_{sw} = m_{sw,o} - m_{yield} \tag{7}$$

where, S_{sw} is the absorbed portion of solar energy by the saline water, and $Q_{C,\,b\text{-}sw}$ is the convection heat transfer from the basin to the saline water, which are defined as follows.

$$S_{sw} = \tau_g\,\alpha_{sw}\,I A_P \tag{7a}$$

$$Q_{C,\,b\text{-}sw} = h_{b\text{-}sw}\,A_b(T_b - T_{sw}) \tag{7b}$$

The basins in the DSSS-SAHC and the CDSSS absorb solar radiation and heat the saline water and the basin insulation, respectively, through convection and conduction heat transfer as follows.

$$m_b\,C_b\frac{dT_b}{dt} = S_b - Q_{C,\,b\text{-}sw} - Q_{Cd,\,b\text{-}i} \tag{8}$$

where, S_b is the absorbed portion of solar energy by the basin, and $Q_{Cd,\,b\text{-}i}$ is the conduction losses from the basin to the insulation, which are defined as follows.

$$S_b = \tau_g\,\tau_{sw}\,\alpha_b\,I A_P \tag{8a}$$

$$Q_{Cd,\,b\text{-}i} = \frac{2\frac{k_b \times k_i}{k_b + k_i}\,A_b\,(T_b - T_i)}{\frac{L_b + L_i}{2}} \tag{8b}$$

The basins insulations in the DSSS-SAHC and the CDSSS losses thermal energy to the ambient environment by convection and radiation.

$$m_i\,C_i\frac{dT_i}{dt} = Q_{Cd,\,b\text{-}i} - Q_{R,\,i\text{-}sky} - Q_{C,\,i\text{-}amb} \tag{9}$$

where, $Q_{R,\,i\text{-}sky}$ is radiative losses from the insulation to the sky, and $Q_{C,\,i\text{-}amb}$ is the convective losses from the insulation to the surrounding ambient, which are defined as follows.

$$Q_{R,\,i\text{-}sky} = \sigma\,\varepsilon_i\,A_i\,(T_i^4 - T_{sky}^4) \tag{9a}$$

$$Q_{C,\,i\text{-}amb} = h_{i\text{-}amb}\,A_i\,(T_i - T_{amb}) \tag{9b}$$

2.3 Thermal Performance of CDSSS and DSSS-SAHC

The overall thermal efficiency of the DSSS-SAHC is expressed as

$$\eta = \eta_{still} + \eta_{heater} = \frac{\sum_{t=0}^{t=t_{op}}\left((m_{yield} \times H) + (m_a \times C_a \times \Delta T_a)\right)}{\sum_{t=0}^{t=t_{sun}} I\,A} \tag{10}$$

While the overall thermal efficiency of the CDSSS is

$$\eta_{still} = \frac{\sum_{t=0}^{t=t_{op}}(m_{yield} \times H)}{\sum_{t=0}^{t=t_{sun}} I\,A} \tag{11}$$

3. Results and Discussion

3.1 Weather Conditions

As shown in Fig 3, the weather conditions in Sakaka, Saudi Arabia (located at 29.9° N, 39.3° E) were measured on September 25th. During the day, the solar flux, incident on a 30° inclined plane, increased gradually from the morning until it reached a maximum of approximately 1050 W/m^2 around noon. Consequently, the temperature increased as well to its highest point of 41°C two hours afternoon. Both the solar flux and the surrounding temperature dropped off in the afternoon while the wind speed was observed to vary during the day around an average wind speed of 1.5 m/s.

The measured solar intensity was correlated with respect to time as a fourth-degree polynomial function as follows.

$$I(t) = 321194t^4 - 645790t^3 + 451032t^2 - 127219t + 12551 \tag{12}$$

Similarly, the measured ambient temperature was correlated with respect to time as a third-degree polynomial function as follows.

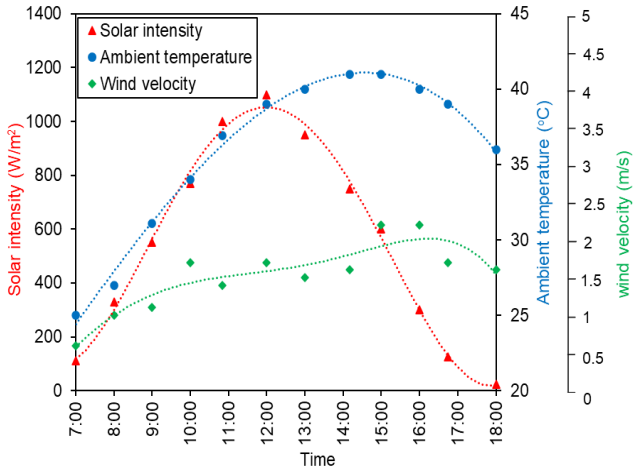

Fig 3. Weather conditions at Sakaka, KSA on September 25th.

$$T_{amb}(t) = -193.96t^3 + 124.08t^2 + 63.724t + 0.0746 \quad (13)$$

The correlated weather data were employed in the numerical model to investigate the performances of the DSSS-SAHC and the CDSSS.

3.2 Overall Performance of DSSS-SAHC

Fig 4 compares the temperature distributions inside the DSSS-SAHC for air flows of 0.01 and 0.1 kg/s (representing natural and forced air circulations, respectively) with those inside the CDSSS based on the weather conditions in Fig 3. In general, the components' temperatures of the CDSSS are lower than those of the DSSS-SAHC at both 0.01 and 0.1 kg/s air flows. This is due to the presence of the SAHC, which reduces the losses from the glass cover (g_2) to the ambient surroundings and, consequently, results in conserving thermal energy within the components of the DSSS-SAHC. Consistently, the components temperatures of the DSSS-SAHC for the case of 0.1 kg/s air flow are lower than those for the case of 0.01 kg/s. This can be attributed to the increased cooling effect of the air as its flow rate increases. However, the air exit temperature (T_2) is slightly higher for the case of 0.01 kg/s air flow than for the case of 0.1 kg/s due to the inverse proportion between the flow rate and the air temperature difference.

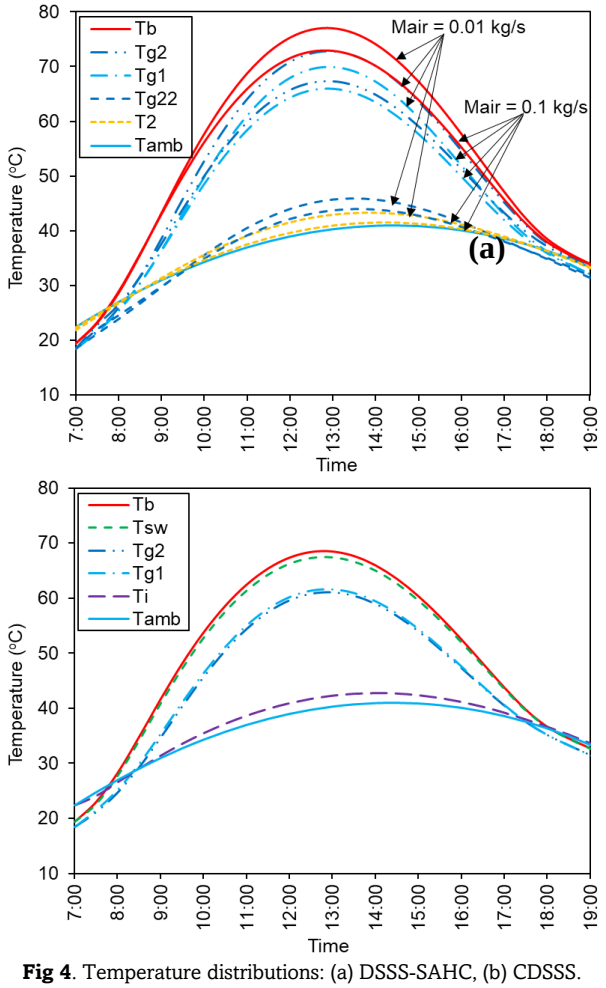

Fig 4. Temperature distributions: (a) DSSS-SAHC, (b) CDSSS.

Fig 5 compares the distillate yield and the overall thermal performance of the DSSS-SAHC at air flows of 0.01 and 0.1 kg/s to those of the CDSSS. The yields of the DSSS-SAHC at both air flows are marginally greater than that of the CDSSS. This is because of the air cooling of the back cover (g_2) by the air flow inside the SAHC. In addition, the yield of the DSSS-SAHC at an air flow of 0.1 kg/s is insignificantly greater than that at an air flow of 0.01 kg/s due to the increase in the air cooling of the back cover with the increase in the air flow rate. However, the overall efficiency of the DSSS-SAHC at an air flow of 0.1 kg/s is approximately 9% greater than that at an air flow of 0.01 kg/s. This is attributed to the increase in the efficiency of the SAHC with the increase in the air flow, which adds up to the overall efficiency of the DSSS-SAHC. Furthermore, the efficiencies of the DSSS-SAHC at 0.1 kg/s and 0.01 kg/s are approximately 15% and 6% greater than that of the CDSSS. This is because the recovery of the thermal losses of the DSSS in heating air inside the SAHC as an additional product contributes to the overall efficiency of the DSSS-SAHC.

The water distillates on the glass covers (g_1) and (g_2) of the DSSS-SAHC at air flows of 0.01 and 0.1 kg/s are illustrated in Fig 6 and compared to those of the CDSSS. The presence of the SAHC reduced the thermal losses to the surrounding ambient and, hence, reduced the amount of distillate condensed on the glass cover (g_2) of the the DSSS-SAHC at both flows of 0.01 and 0.1 kg/s compared to the CDSSS. Consequently, the DSSS-SAHC distillates condensed on the glass cover (g_1) are greater than that of the CDSSS. In addition, as the temperature of the glass cover (g_2) of the DSSS-SAHC decreased with the increase in the air flow from 0.01 to 0.1 kg/s, the distillate on the glass cover (g_2) increased with the increase in the air flow at the expense of the distillate condensed on the glass cover (g_1) decreased.

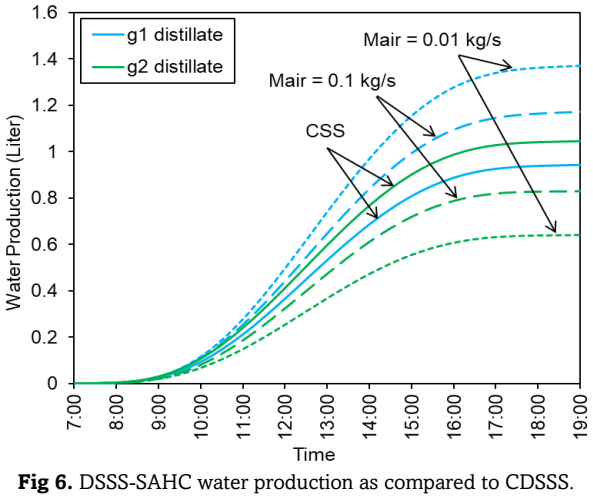

Fig 6. DSSS-SAHC water production as compared to CDSSS.

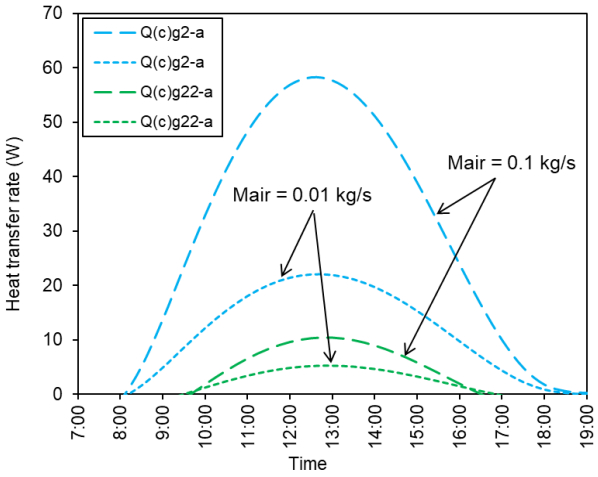

Fig 7. Air heat gain at various air flow rates.

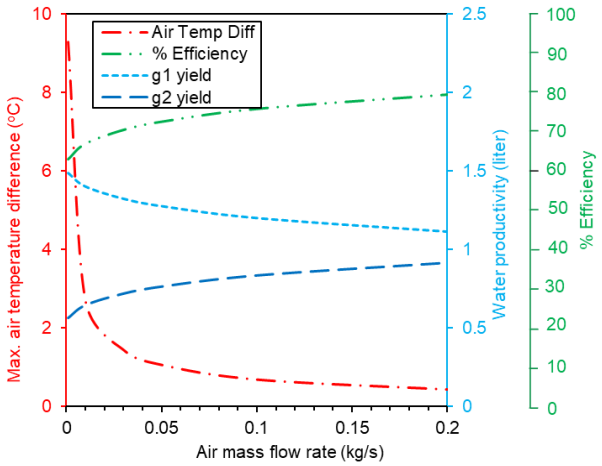

Fig 9. Influence of air flow rate on the overall performance of DSSS-SAHC.

Additionally, the air heat gain within the SAHC is shown in Fig 7 at air flows of 0.1 and 0.01 kg/s. At an air flow of 0.1 kg/s, the air heat gains by convection from glass covers (g_{22}) and (g_2) are respectively about double and three times those at an air flow of 0.01 kg/s as a result of the increase in the convection heat transfer from the glass covers to then flowing air with the increase in the air flow rate. This, in turn, explains the increase in the efficiency of the DSSS-SAHC with the increase in the air flow rate.

Fig 8 compares the energy losses from the DSSS-SAHC to the ambient surroundings at air flows of 0.1 and 0.01 kg/s to those from the CDSSS. It is shown that the losses from the glass cover (g_{22}) of the DSSS-SAHC at air flows of 0.1 and 0.01 kg/s are less than half the losses from the glass cover (g_2) of the CDSSS. This can be attributed to the partial recovery of these losses by the flowing air in the SAHC. In addition, the losses at an air flow of 0.01 kg/s are greater than those at an air flow of 0.1 kg/s as the bigger the flow rate, the bigger the recovery of the thermal losses. Consequently, as a result of the reduction in the losses from the glass cover (g_2), the losses from the glass cover (g_1) of the DSSS-SAHC at air flows of 0.1 and 0.01 kg/s increased as compared to those in the CDSSS. Furthermore, the difference between the losses from the basin in the DSSS-SAHC at air flows of 0.1 kg/s and 0.01 kg/s and those from the CDSSS is negligible as the temperatures of the basins of the DSSS-SAHC and the CDSSS are almost equal.

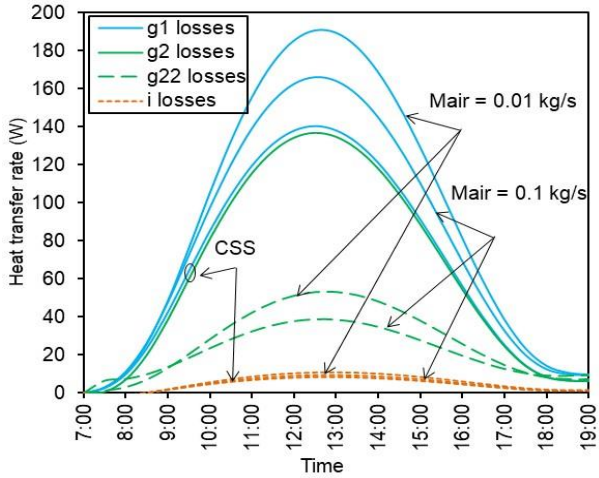

Fig 8. Losses from glass covers and basin insulation to surrounding ambient.

3.3 Effect of Air Flow Rate on the Overall Performance

The overall performance of the DSSS-SAHC at different air flows and based on the weather conditions presented in Fig 3 is shown in Fig 9. Increasing the air flow (the transition from natural to forced circulation) decreased the air temperature difference at the SAHC's exit exponentially, increased the overall thermal efficiency by about 26 %, and reduced the distillate condensed on the glass cover (g_2) by about 0.36 liters while increased the distillate condensed on the glass cover (g_1) by nearly the same amount. Nevertheless, for all air flows, the distillate condensed on the glass cover (g_1) is greater than that on the cover (g_2). The reason for that is the presence of the SAHC decreased the release of the thermal losses from the cover (g_2) to the ambient surroundings as compared to those from the cover (g_1), which led to a substantial increase in the temperature of (g_2) over that of (g_1). As a result, the temperature difference between the saline water and the glass cover is greater in the case of (g_1) as compared to (g_2), and hence the distillate condensation on (g_1) is greater than that on (g_2). In addition, the decrease in the temperature of (g_2) as the air flow rate increases caused an increase in the distillate condensation on (g_2) at the expense of that on (g_1). Moreover, due to the inverse proportion between the air flow rate and the air temperature, the increase in the air flow rate significantly reduced the air exit temperature despite the increase in the air heat gain by the air due to the increase in its flow rate.

3.4 Effect of Weather Conditions on the Overall Performance

The solar irradiance intensity plays a vital role in the performance of the DSSS-SAHC as the thermal input to the still. Fig 10. depicts the overall performance of the DSSS-SAHC at different solar irradiance intensities and air flows of 0.01 and 0.1 kg/s. The increase in the solar irradiance intensity from 950 to 1150 W/m^2 increased the still productivity by about 0.7 liters. This is attributed to the increase in the energy input to the still, which agrees with the results of the numerical study conducted by Fath & Hosny (2002). However, the variation in the air flow had an insignificant effect on water production for various solar intensities. In addition, the air exit temperature difference increased by about 0.6°C and 0.2°C, and the thermal efficiency increased by 1% and 2%, respectively, at air flows of 0.01 and 0.1 kg/s. This is because of the increase in the distillate condensation on the cover (g_2) and, hence, the heat recovery by the air inside the SAHC.

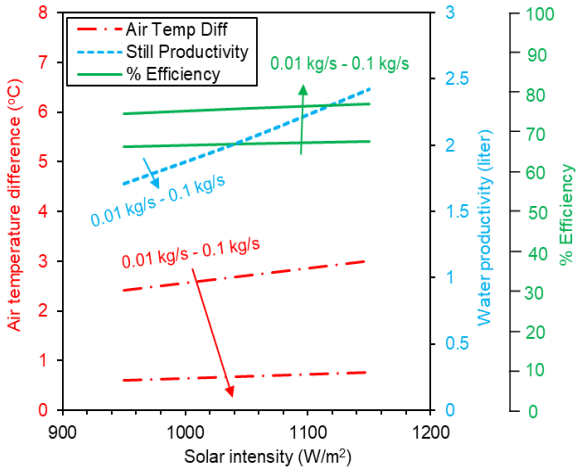

Fig 10. Influence of solar irradiation intensity on the overall performance of DSSS-SAHC.

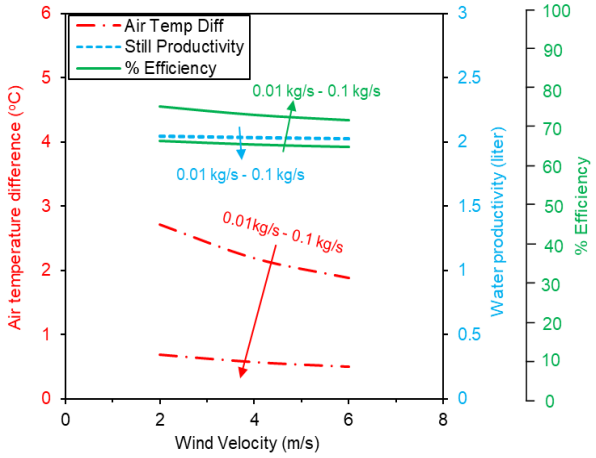

Fig 12. Effect of ambient wind speed on the DSSS-SAHC overall performance.

The ambient surroundings temperature controls heat transfer (thermal losses) between the still and the surroundings. Therefore, the increase in ambient temperature reduces the still's thermal losses. The impact of ambient air temperature on the DSSS-SAHC performance is illustrated in Fig 11. The rise in the ambient temperature from 30 to 50 °C increased the water distillate by 0.13 liters and 0.15 liters, respectively, for air flows of 0.01 and 0.1 kg/s. This is because of the reduction in the thermal losses from the system to the ambient surroundings. This finding is consistent with the numerical results of Fath & Hosny (2002). In addition, the DSSS-SAHC thermal efficiency increased by about 3% at an air flow of 0.01 kg/s and by 5% at an air flow of 0.1 kg/s as a result of the increase in distillate production. However, the exit air temperature changed marginally for both air flows with the increase in the entering ambient air. The ambient wind influences the still energy losses to the ambient and, consequently, the DSSS-SAHC overall performance. Fig 12 illustrates the effect of increasing the ambient wind speed on the performance of the DSSS-SAHC at air flows of 0.01 and 0.1 kg/s. As shown in the figure, the rise in the wind velocity from 2 to 6 m/s reduced the thermal efficiency of the DSSS-SAHC by 2% and 4%, respectively, at air flows of 0.01 and 0.1 kg/s. This can be attributed to the increase in the losses from the DSSS-SAHC to the ambient surroundings with the rise in wind velocity. However, for both air flows, water production, and exit air temperature decreased insignificantly as a result of the marginal increase in the thermal losses from the still to the ambient surroundings. The influence of the ambient wind velocity on the overall performance of the DSSS-SAHC agrees with the experimental results of Castillo-Téllez *et al.* (2015).

3.5 Effect of Basin's Water Height

Finally, the effect of the DSSS-SAHC basin's water height is shown in Fig 13. At air flows of 0.01 to 0.1 kg/s, increasing the basin's water height from 6 mm to 14 mm insignificantly reduced the DSSS-SAHC's water production, exit air temperature, and thermal efficiency. The reason is that increasing the mass of the water in the basin led to a marginal decrease in its temperature and, hence, the heat and mass transfer from the water to the glass covers, which, in turn, reduced the distillate condensation and the thermal losses recovery by the air in the SAHC. For example, a difference in air temperature of about 2°C was predicted when decreasing air flow from 0.1 to 0.01 kg/s at a water height of 6 mm, while the difference decreased slightly at a water height of 12 mm due to the reduction in the temperatures across the SAHC. Nevertheless, when increasing air flow from 0.01 to 0.1 kg/s at a water height of 6 mm, a difference in thermal efficiency of approximately 9% was predicted, while the difference grew slightly at a water height of 12 mm as a result of reducing the losses from the system. The influence of the basin's water height

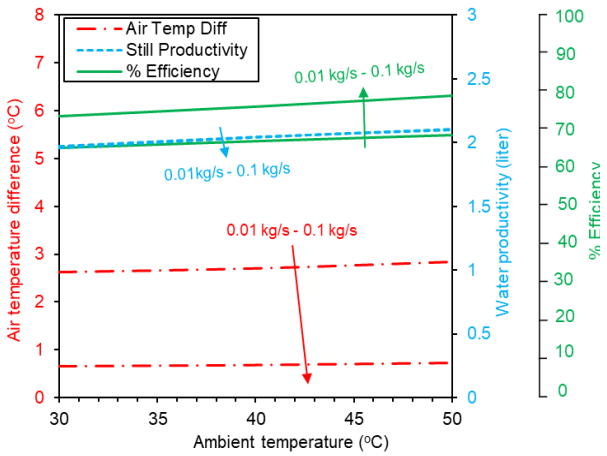

Fig 11. Influence of ambient air temperature on the DSSS-SAHC overall performance.

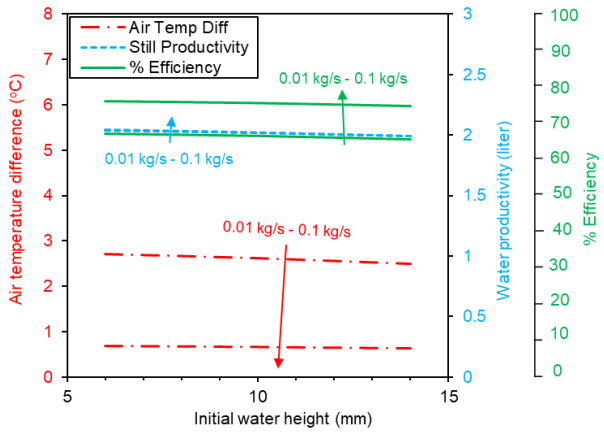

Fig 13. impact of initial basin water height on the DSSS-SAHC overall performance.

Table 2
The performance of the DSSS-SAHC as compared to other passive DSSSs described in the literature.

DSSS design modification	Distillate production ($kg/m^2.day$)	Thermal performance (%)	Reference
External reflector	4.98	69%	Gnanaraj & Velmurugan (2022)
Sensible heat storage material	3.76	54%	
Finned basin	2.7	35%	Tuly *et al.* (2021)
Circular finned basin	1.5	27%	Jani & Modi (2019)
Truncated conic finned basin	1.84	58.6%	Kaviti *et al.* (2021)
Parabolic finned basin	1.7	52.8%	
Elevated basin	4.15	40%	Hussen *et al.* (2023)
Al_2O_3 nanofluid	7.46	50%	Sahota & Tiwari (2016)
TiO_2 nanofluid	7.05	46%	
Gravel, carbon black nanofluid, and glass cooling	4.2	46.9%	Elmaadawy *et al.* (2021)
Gravel, black wick, and glass cooling	4.37	48.7%	
Gravel, black wick, carbon black, and glass cooling	4.91	59.5%	
Stepped DSSS, and linen wicks	3.26	40.8%	Sharshir *et al.* (2020)
Stepped DSSS, and carbon black nanoparticles	3.55	49.9%	
Stepped DSSS, linen wicks, and carbon black nanoparticles	4.46	60.2%	
Prismatic basin, linen wicks, and glass cooling	8.2	49%	Zayed *et al.* (2023)
Solar air heater condenser	4.1	67% - 76%	Present study

is consistent with the consecutive research work conducted by Murugavel *et al.* (2008 and 2010).

3.6 Comparing the Present Study to Previous Studies

In addition, Table 2 compares the performance of the current DSSS-SAHC to that of other passive DSSSs in the literature. The majority of the studies cited in the table were concerned with increasing the distillate production of the DSSS through increasing the solar energy input by the use of an external reflector (Gnanaraj & Velmurugan, 2022), enhancing the evaporation of saline water by insertion of nanoparticles (Sahota & Tiwari, 2016 and Sharshir *et al.*, 2020) and by covering the basin with black wick (Elmaadawy *et al.*, 2021 and Sharshir *et al.*, 2020), increasing the evaporation area by incorporating various shapes of fins (Tuly *et al.*, 2021, Jani & Modi, 2019, and Kaviti *et al.*, 2021), storing solar energy to extend distillate production after sunset (Gnanaraj & Velmurugan, 2022 and Elmaadawy *et al.*, 2021), and enhancing distillate condensation by glass cooling (Elmaadawy *et al.*, 2021 and Zayed *et al.*, 2023). However, the current study focused on recovering the inevitable thermal losses of the simplest conventional DSSS in heating ambient air in order to produce both distillate water and hot air simultaneously for the same solar energy input to the still. In addition, the current study did not adopt any of the aforementioned modifications, which explains the recess in the distillate production of the current study as compared to most of the studies listed in Table 2. Even though, the distillate productivity of the current study is greater than those of Tuly *et al.* (2021), Jani & Modi (2019), and Kaviti *et al.* (2021). However, recovering the thermal losses of the DSSS in producing hot air, in the current study, significantly contributed to enhancing the overall thermal efficiency of the current DSSS-SAHC. This can be recognized by the superiority of the overall thermal efficiency of the current DSSS-SAHC over those of the DSSSs cited in Table 2.

4. Conclusions

A combined DSSS-SAHC was numerically modelled, and its thermal performance under measured weather conditions of Sakaka, Saudi Arabia (located at 29.9° N, 39.8° E) was investigated and compared to that of CDSSS of the same basin area. The DSSS-SAHC was created by replacing the back cover of CDSSS with a glass air heater in an effort to recover still thermal losses in heating air. Air flows between 0.01 and 0.1 kg/s were considered to account for both natural and forced air circulation, respectively. The efficiency of the DSSS-SAHC was about 15% and 6% greater than that of the CDSSS, respectively, for air flows of 0.1 and 0.01 kg/s despite the distillate of the DSSS-SAHC was insignificantly greater than that of the CDSSS at both air flows. In addition, the bigger the air flow rate, the less the exit air temperature. Moreover, the DSSS-SAHC produced significantly more water distillate with an increase in solar irradiance, while its efficiency increased marginally. In contrast, the distillate increased insignificantly as the ambient temperature rose, whereas the efficiency increased by about 3% to 5%. In addition, faster wind speed reduced the DSSS-SAHC efficiency by about 2% to 4% without significantly affecting the water distillate or exit air temperature. Similarly, increasing the initial basin water level had a negligible impact on the water distillate, efficiency, and air exit temperature.

Acknowledgment

The author extends his appreciation to the Deputyship for Research & Innovation, Ministry of Education in Saudi Arabia for funding this work through the project number "375213500". The author would like to extend his sincere appreciation to the central laboratory at Jouf University for supporting this study.

Nomenclature

A	Area
C	Specific heat
F	Radiation view factor

h	Heat transfer coefficient
H	Latent heat of evaporation
I	Solar Irradiance intensity
k	Thermal conductivity
L	Thickness
m	Mass
P	Partial pressure
Q	heat transfer rate
S	Absorbed solar radiation
T	Temperature
t	Time

Greek Letters

D	Difference
a	Surface absorptivity
e	Surface emissivity
□	Efficiency
s	Stefan-Boltzmann constant
t	Surface transmissivity

Subscripts

a	Air
amb	Ambient environment
b	Basin
C	Convection heat transfer
Cd	Conduction heat transfer
e	Evaporation
g, g1, g2, g22	Glass cover
heater	Solar air heater
i	Basin insulation
o	Initial state
P	Projection
op	Operation duration
R	Radiation heat transfer
sky	Sky temperature
still	Solar still
sun	day time
sw	Saline water
yield	Water distillate

References

Abdullah, A.S., Alarjani, A., Abou Al-sood, M.M., Omara, Z.M., Kabeel, A.E. & Essa, F.A. (2019). Rotating-wick solar still with mended evaporation technics: Experimental approach, *Alexandria Engineering Journal,* 58, 1449-1459. https://doi.org/10.1016/j.aej.2019.11.018

Agrawal, R. & Singh, K.D.P. (2021). Performance evaluation of double slope solar still augmented with binary eutectic phase change material and steel wool fibre, *Sustain. Energy Technol. Assessments*, 48, 101597. https://doi.org/10.1016/j.seta.2021.101597

Ahmed, H.M., Alshutal, F.S. & Ghaleb, I.G. (2014). Impact of Different Configurations on Solar Still Productivity, *J. Adv. Sci. Eng. Res.*, 4(2), 118-126. http://www.sign-ific-ance.co.uk/index.php/JASER/article/viewFile/762/1442

Alwan, N.T., Shcheklein, S.E. & Ali O.M. (2020). Experimental investigation of modified solar still integrated with solar collector, *Case Studies in Thermal Engineering*, 19, 100614. https://doi.org/10.1016/j.csite.2020.100614

Belhadj, M.M., Bouguettaia, H., Marif, Y. & Zerrouki, M. (2015). Numerical study of a double-slope solar still coupled with capillary film condenser in south Algeria, *Energy Conversion and Management*, 94, 245–252. https://doi.org/10.1016/j.enconman.2015.01.069

Castillo-Téllez, M., Pilatowsky-Figueroa, I., Sánchez-Juárez, Á. & Fernández-Zayas, J. L. (2015). Experimental study on the air velocity effect on the efficiency and fresh water production in a forced convective double slope solar still, *Applied Thermal Engineering,* 75, 1192-1200. https://doi.org/10.1016/j.applthermaleng.2014.10.032

Dwivedi, V.K. & Tiwari, G.N. (2010). Experimental validation of thermal model of a double slope active solar still under natural circulation mode, *Desalination,* 250, 49-55. https://doi.org/10.1016/j.desal.2009.06.060

Elgendi, M., Selim, M.Y.E., Aldhaheri, A., Alshehhi, W., Almarshoodi, H. & Alhefeiti, A. (2022). Design procedures for a passive pyramid solar still with an automatic feed water system, *Alexandria Engineering Journal,* 61, 6419-6431. https://doi.org/10.1016/j.aej.2021.12.002

Elmaadawy, K., Kandeal, A.W., Khalil, A., Elkadeem, M.R., Liu, B., Sharshir, S.W. (2021). Performance improvement of double slope solar still via combinations of low cost materials integrated with glass cooling, *Desalination,* 500, 114856. https://doi.org/10.1016/j.desal.2020.114856

El-Maghlany, W.M. (2015). An approach to optimization of double slope solar still geometry for maximum collected solar energy, *Alexandria Engineering Journal*, 54(4), 823-828. https://doi.org/10.1016/j.aej.2015.06.010

Essa, F.A., Abd Elaziz, M. & Elsheikh, A.H. (2020). An enhanced productivity prediction model of active solar still using artificial neural network and Harris Hawks optimizer, *Applied Thermal Engineering,* 170, 115020. https://doi.org/10.1016/j.applthermaleng.2020.115020

Fallahzadeh, R., Aref, L., Avargani, V.M. & Gholamiarjenaki, N. (2020). An experimental investigation on the performance of a new portable active bubble basin solar still, *Applied Thermal Engineering,* 181, 115918. https://doi.org/10.1016/j.applthermaleng.2020.115918

Fath, H.E.S. & Hosny, H.M. (2002). Thermal performance of a single-sloped basin still with an inherent built-in additional condenser, *Desalination,* 142, 19-27. https://doi.org/10.1016/S0011-9164(01)00422-2

Gnanaraj, S.J.P. & Velmurugan, V. (2022). Experimental investigation on the performance of modified single basin double slope solar stills, *International Journal of Ambient Energy*, 43(1), 206-215. https://doi.org/10.1080/01430750.2019.1636861

Hedayati-Mehdiabadi, E., Sarhaddi, F. & Sobhnamayan, F. (2020). Exergy performance evaluation of a basin-type double-slope solar still equipped with phase-change material and PV/T collector, *Renew. Energy*, 145, 2409-2425. https://doi.org/10.1016/j.renene.2019.07.160

Hussen, H.M., Younes, M.M., Alawee, W.H., Abdullah, A.S., Mohammed, S.A., Atteya, T.E.M., Abbas, F. & Omara, Z.M. (2023). An experimental comparison study between four different designs of solar stills, *Case Studies in Thermal Engineering,* 44, 102841. https://doi.org/10.1016/j.csite.2023.102841

Jani, H.K. & Modi, K.V. (2019). Experimental performance evaluation of single basin dual slope solar still with circular and square cross-sectional hollow fins. *Sol. Energy*, 179, 186-194. https://doi.org/10.1016/j.solener.2018.12.054

Kabeel, A.E., Harby, K., Abdelgaied, M. & Eisa, A. (2020). Performance of the modified tubular solar still integrated with cylindrical parabolic concentrators, *Solar Energy*, 204, 181-189. https://doi.org/10.1016/j.solener.2020.04.080

Kaviti, A.K., Naike, V.R., Ram, A.S. & Thakur, A.K. (2022). Energy and exergy analysis of a truncated and parabolic finned double slope solar stills, *International Journal of Ambient Energy*, 43(1), 6210-6223. https://doi.org/10.1080/01430750.2021.2009368

Kumbhar, S.V. (2019). Double slope solar still distillate output data set for conventional still and still with or without reflectors and PCM using high TDS water samples, *Data in brief*, 24, 103852. https://doi.org/10.1016/j.dib.2019.103852

Maheswari, K.S., Mayandi, K., Joe Patrick Gnanaraj, S. & Appadurai, M. (2022). Effect of transparent glass cover material on double slope solar still productivity, *Mater. Today: Proc.*, 62(8), 5415-5419. https://doi.org/10.1016/j.matpr.2022.03.702

Mevada, D., Panchal, H., Ahmadein, M., Zayed, M.E., Alsaleh, N.A., Djuansjah, J., Moustafa, E.B., Elsheikh, A.H. & Sadasivuni, K.K. (2022). Investigation and performance analysis of solar still with energy storage materials: An energy- exergy efficiency analysis, *Case Studies in Thermal Engineering*, 29, 101687. https://doi.org/10.1016/j.csite.2021.101687

Modi, K. & Jani, H. (2021). Experimental and theoretical assessment of dual-slope single-basin solar still with the circular cross-sectional hollow-fins. *Cleaner Engineering and Technology*, 4, 100231. https://doi.org/10.1016/j.clet.2021.100231

Modi, K.V., Nayi, K.H. & Sharma, S.S. (2020). Influence of water mass on the performance of spherical basin solar still integrated with parabolic reflector, *Groundwater for Sustainable Development*, 10, 100299. https://doi.org/10.1016/j.gsd.2019.100299

Modi, K.V., Patel, U.N., Patel, S.J., Patel, J.N. & Patel, S.R. (2022).Efficacy of partially and fully submerged circular cross-section metal hollow-fins and black cotton cloth wick-segments on a single-basin dual-slope solar still, *Journal of Cleaner Production,* 344, 131059. https://doi.org/10.1016/j.jclepro.2022.131059

Morad, M.M., El-Maghawry, H.A.M. & Wasfy, K.I. (2015). Improving the double slope solar still performance by using flat-plate solar collector and cooling glass cover, *Desalination*, 373, 1-9. https://doi.org/10.1016/j.desal.2015.06.017

Murugavel, K.K. & Srithar, K. (2011). Performance study on basin type double slope solar still with different wick materials and minimum mass of water, *Renewable Energy*, 36, 612-620. https://doi.org/10.1016/j.renene.2010.08.009

Murugavel, K.K., Chockalingam, Kn.K.S.K. & Srithar, K. (2008). An experimental study on single basin double slope simulation solar still with thin layer of water in the basin, *Desalination,* 220, 687-693. https://doi.org/10.1016/j.desal.2007.01.063

Murugavel, K.K., Sivakumar, S., Ahamed, R.J., Chockalingam, S.K. & Srithar, K. (2010). Single basin double slope solar still with minimum basin depth and energy storing materials, *Appl. Energy,* 87, 514-523. https://doi.org/10.1016/j.apenergy.2009.07.023

Patel, S.K., Kumar, B., Pal, P., Dev, R. & Singh, D. (2020). Production of potable water from Gomti River by using modified double slope solar still with external mounted reflectors, *Solar Energy*, 209, 576-589. https://doi.org/10.1016/j.solener.2020.09.036

Raihananda, F.A., Philander, E., Lauvandy, A.F., Soelaiman, T.A.F., Budiman, B.A., Juangsa, F.B. & Sambegoro, P. (2021). Low-cost floating solar still for developing countries: Prototyping and heat-mass transfer analysis, *Results in Engineering*, 12, 100300. https://doi.org/10.1016/j.rineng.2021.100300

Rajaseenivasan, T. & Murugavel, K. K. (2013). Theoretical and experimental investigation on double basin double slope solar still, *Desalination*, 319, 25-32. https://doi.org/10.1016/j.desal.2013.03.029.

Sahota, L. & Tiwari, G.N. (2016). Effect of nanofluids on the performance of passive double slope solar still: A comparative study using characteristic curve, *Desalination*, 388, 9-21. https://doi.org/10.1016/j.desal.2016.02.039.

Sathyamurthy, R., Kabeel, A.E., Balasubramanian, M., Devarajan, M., Sharshir, S.W. & Manokar, A.M. (2020). Experimental study on enhancing the yield from stepped solar still coated using fumed silica nanoparticle in black paint, *Materials Letters,* 272, 127873. https://doi.org/10.1016/j.matlet.2020.127873

Sharshir, S.W., Eltawil, M.A., Algazzar, A.M., Sathyamurthy, R. & Kandeal, A.W. (2020). Performance enhancement of stepped double slope solar still by using nanoparticles and linen wicks: Energy, exergy and economic analysis, *Applied Thermal Engineering,* 174, 115278. https://doi.org/10.1016/j.applthermaleng.2020.115278

Taamneh, Y., Manokar, A.M., Thalib, M.M., Kabeel, A.E., Sathyamurthy, R. & Chamkha, A.J. (2020). Extraction of drinking water from modified inclined solar still incorporated with spiral tube solar water heater, *Journal of Water Process Engineering*, 38, 101613. https://doi.org/10.1016/j.jwpe.2020.101613

Tabrizi, F.F., Dashtban, M., Moghaddam, H. & Razzaghi, K. (2010). Effect of water flow rate on internal heat and mass transfer and daily productivity of a weir-type cascade solar still, *Desalination,* 160, 239-427. https://doi.org/10.1016/j.desal.2010.03.037

Tiwari, G.N., Mukherjee, K., Ashok, K.R. & Yadav, Y.P. (1986). Comparison of various designs of solar stills, *Desalination*, 60, 191-202. https://doi.org/10.1016/0011-9164(86)90008-1

Tuly, S.S., Rahman, M.S., Sarker, M.R.I. & Beg, R.A. (2021). Combined influence of fin, phase change material, wick, and external condenser on the thermal performance of a double slope solar still. *J. Clean. Prod.*, 287, 125458. https://doi.org/10.1016/j.jclepro.2020.12545

Zayed, M.E., Kamal, A., Diab, M.R., Essa, F.A., Muskens, O.L., Fujii, M. & Elsheikh, A.H. (2023). Novel Design of Double Slope Solar Distiller with Prismatic Absorber Basin, Linen Wicks, and Dual Parallel Spraying Nozzles: Experimental Investigation and Energic–Exergic-Economic Analyses, *Water*, 15, 610. https://doi.org/10.3390/w15030610